

Sequential Deep Trajectory Descriptor for Action Recognition with Three-stream CNN

Yemin Shi^{1,2}, Yonghong Tian^{1,2*}, Yaowei Wang^{3*}, Tiejun Huang^{1,2}

¹ National Engineering Laboratory for Video Technology, School of EE&CS, Peking University, Beijing, China

² Cooperative Medianet Innovation Center, China

³ School of Information and Electronics, Beijing Institute of Technology, Beijing, China

Abstract—Learning the spatial-temporal representation of motion information is crucial to human action recognition. Nevertheless, most of the existing features or descriptors cannot capture motion information effectively, especially for long-term motion. To address this problem, this paper proposes a long-term motion descriptor called sequential Deep Trajectory Descriptor (sDTD). Specifically, we project dense trajectories into two-dimensional planes, and subsequently a CNN-RNN network is employed to learn an effective representation for long-term motion. Unlike the popular two-stream ConvNets, the sDTD stream is introduced into a three-stream framework so as to identify actions from a video sequence. Consequently, this three-stream framework can simultaneously capture static spatial features, short-term motion and long-term motion in that video. Extensive experiments were conducted on three challenging datasets: KTH, HMDB51 and UCF101. Experimental results show that our method achieves state-of-the-art performance on the KTH and UCF101 datasets, and is comparable to the state-of-the-art methods on the HMDB51 dataset.

Index Terms—Action recognition, sequential Deep Trajectory Descriptor, sDTD, three-stream framework, long-term motion.

I. INTRODUCTION

ACTION recognition is growing to be a widely-used technique in many applications, such as security surveillance, automated driving, home-care nursing and video retrieval. Generally speaking, action recognition aims at identifying the actions or behaviors of one or more persons from a video sequence. An action is typically represented in some consecutive video frames rather than one isolated frame. Naturally, motion information is highly discriminative to detect, understand and recognize actions from a video. Thus how to efficiently learn the effective spatial-temporal representation of motion information is crucial to human action recognition.

In recent years, many studies (e.g., [1], [2], [3], [4]) made their efforts on representing an action with low-level visual features extracted from video frames and optical flow fields, consequently achieving a significant progress. For example, SIFT [5] was extended to 3D-SIFT [6] and applied to action recognition. The work [7] extracted Histogram of Oriented Gradients (HOG) [8] and Histogram of Optical Flow (HOF) at each spatial-temporal interest point, and then encoded features

with Bag of Features (BoF). In order to capture the motion information more effectively, Wang *et al.* [1] proposed a method to extract dense trajectories by sampling and tracking dense points from each frame in multiple scales. They also extracted HOG, HOF and Motion Boundary Histogram (MBH) [9] at each point. The combination of these features was shown to further boost the final performance. The improved version of dense trajectories [2] also considers the camera motion estimation and then applies the BoF or Fisher vector [10] to derive the final representation for each video. In [11], dense trajectories are employed in a joint learning framework to simultaneously identify the spatial and temporal extents of the actions of interest in training videos. However, most of these methods typically could not deal with long-term action, e.g., people hovering or slow walking.

Convolutional Neural Network (CNN) has shown a great success recently and achieves state-of-the-art performance on various tasks (e.g., [12], [13], [14], [15], [16], [17], [18], etc.). It has been proven empirically that the features learnt from CNN are much better than the hand-crafted features like SIFT. In order to transfer CNN from images to videos, several models [13], [19], [20], [21] have been proposed. To capture the spatial-temporal representation from a video, Ji *et al.* [22] extended the traditional CNN to 3D-CNN, which gets inputs from multiple channels and performs 3D convolution. However, it achieved lower performance compared with the hand-crafted representation [2]. A two-stream ConvNets approach was proposed in [3] by incorporating spatial and motion networks and pre-training these networks on the large ImageNet dataset, consequently achieving the state-of-the-art performance. After that, Wang *et al.* [23] successfully trained very deep two-stream ConvNets on the UCF101 dataset. In their two-stream ConvNets, the spatial ConvNet operates on individual frames and performs action recognition as an image classification task. Unlike the spatial ConvNet, the motion ConvNet takes several consecutive optical flow displacement fields as its input to represent the motion between video frames. Typically, it operates on a $2L$ -channel stacked optical flow images, where L is the number of frames in the window, consequently modelling the short-term motion. However, the long-term dependence of frames is still ignored in two-stream ConvNets.

Unlike these pure deep models, the work [15] proposed trajectory-pooled deep-convolutional descriptor (TDD), which shares the merits of both hand-crafted features and deeply-learned features. Hasan *et al.* [24] proposed a continuous activity learning framework for streaming videos, which intricately ties together deep hybrid feature models and active learning. To address the cross-modal video retrieval task, Pang *et al.* [25] presented a multi-pathway Deep Boltzmann Machine (DBM) dealing with low-level features of various types, which learns multi-modal signals coupled with emotions and semantics. Nevertheless, none of these models have the potential for capturing long-term dependence.

In our previous work [19], we proposed a Deep Trajectory Descriptor (DTD) for action recognition. We extracted dense trajectories from multiple consecutive frames and then projected them onto a two-dimensional plane. This resulted in a ‘‘Trajectory Texture’’ image which could effectively characterize the relative motion in these frames. Then, CNN was utilized to learn a more compact and powerful representation of dense trajectories, just like learning the appearance texture features from an image. However, when the dense trajectories overlap too much (denoted as the overwriting problem), it will be hard for DTD to learn a good representation.

More recently, the Long Short Term Memory networks (LSTMs), a special kind of Recurrent Neural Networks (RNNs), was introduced to model long-term actions. Yue-Hei *et al.* [26] and Donahue *et al.* [4] proposed their own recurrent networks respectively by connecting LSTMs to CNNs. Donahue *et al.* tested their model on activity recognition, image description and video description. Wu *et al.* [13] achieved the state-of-the-art performance by connecting CNNs and LSTMs under their hybrid deep learning framework. Sharma *et al.* [27] introduced the attention technique into LSTMs, which learns to focus selectively on parts of the video frames and classifies videos after a few glimpses.

In these RNN-LSTM networks, however, modeling the long-range dependencies are still problematic in practice. To address this problem, several methods have been proposed recently in the field of Neural Machine Translation (NMT), which aims at translating a sentence from one language to another automatically. The work [14] found that reversing the source sequence and feeding it backwards into the encoder would improve the LSTMs’ performance markedly, because it shortens the path from the decoder to the relevant parts of the encoder. Zaremba *et al.* [28] found that feeding an input sequence twice also would help a network to better memorize things. However, for action recognition, neither reversing the video nor feeding the video twice is efficient.

In this paper, we propose a sequential Deep Trajectory Descriptor (sDTD) to effectively characterize long-term motion in video, consequently facilitating action recognition. A simplified version of dense trajectories is first extracted from multiple consecutive frames to represent the motion from body movement or the relative motion between the camera and objects. Then we project a set of trajectories onto a canvas, consequently resulting in a Trajectory Texture image, and trajectories from each video are converted into a sequence of Trajectory Texture images (as shown in Figure

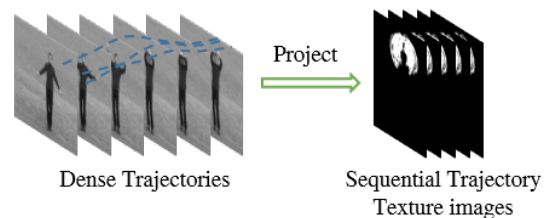


Fig. 1. Trajectories from a video are converted into a sequence of Trajectory Texture images. These images effectively characterize the relative motion in these frames and convert the raw 3D movement into multiple two-dimensional planes.

1). Based on these images, a CNN can be employed to learn a macroscopical representation of motion. In order to model the dependence on the temporal domain, we consider each Trajectory Texture image as a unit and try to model them in the temporal domain with the LSTMs network. As such, videos are violently compressed over the temporal domain, making it easier for LSTMs to learn the long-term dependence.

In order to learn both spatial and motion representation, we also propose a three-stream framework. Our framework is composed of spatial stream, temporal stream and sDTD stream, which are designed to capture spatial feature, short-term feature and long-term feature respectively. The effectiveness of the proposed framework is evaluated on three public datasets: KTH, HMDB51 and UCF101. The experimental results show that our method achieves the state-of-the-art performance on the KTH and UCF101 datasets, and outperforms most methods on the HMDB51 dataset.

The remainder of this paper is organized as follows. In section II, the sequential Deep Trajectory Descriptor (sDTD) is introduced. The three-stream action recognition framework is presented in section III. The experimental results are discussed in section IV. Finally, section V concludes this paper.

A preliminary version of this work has been published in [19]. The main extensions include three aspects. First, we extend the Trajectory Texture image to sequential Trajectory Texture image to reduce the pixel overwriting problem. In order to fully utilize the model pre-trained on the ImageNet dataset, we construct 3-channel Trajectory Texture images along the x and y directions of optical flows and the original direction of motion. Second, a three-stream framework is used for action recognition task, in which GoogLeNet [16] is employed to learn sDTD, and the network is extended with LSTMs so as to model the long-term dependence. Finally, extensive experiments are performed on more datasets so as to evaluate the effectiveness of the proposed method.

II. SEQUENTIAL DEEP TRAJECTORY DESCRIPTOR

Figure 2 illustrates the pipeline of our sequential Deep Trajectory Descriptor (sDTD). Our descriptor first extracts the simplified dense trajectories and then converts these trajectories into sequential Trajectory Texture images. Then, a deep neural network is employed to learn the descriptor for motion. This deep neural network is composed of a CNN part and a LSTM part, where the CNN part aims at learning the

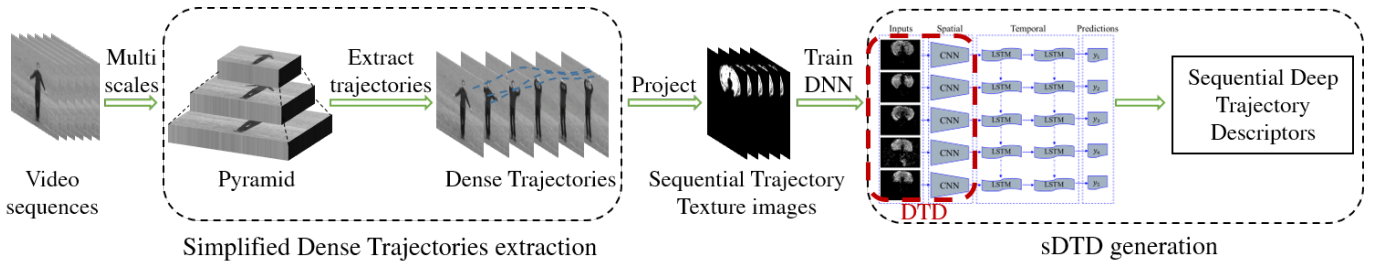


Fig. 2. **The pipeline of sDTD.** The extraction process of sDTD is composed of three steps: (i) extracting the simplified dense trajectories, (ii) converting these trajectories from each video into a sequence of Trajectory Texture images, (iii) learning sDTD with a CNN-RNN network (note that the CNN part features are also called DTD [19]).

spatial features while the LSTM part is designed to capture the temporal features.

A. The Simplified Dense Trajectories

The initial version of dense trajectories was proposed by Wang *et al.* [1]. Basically, it densely samples a set of points from multiple spatial scales on a grid with a step size of W pixels, and then tracks them in multiple spatial scales. Let (x_t, y_t) denote the point p_t at frame t . Then these sampled points are tracked by median filtering in a dense optical flow field $\omega = (u_t, v_t)$, as follows:

$$P_{t+1} = (x_{t+1}, y_{t+1}) = (x_t, y_t) + (\mathcal{M} * \omega_t)|_{(\bar{x}_t, \bar{y}_t)}, \quad (1)$$

where \mathcal{M} is the median filter kernel, $*$ is the convolution operator, and (\bar{x}_t, \bar{y}_t) is the rounded position of (x_t, y_t) . The maximum length of trajectories is set as L frames so as to avoid the drifting problem. A trajectory with too small or too large displacement is also removed. Finally, a trajectory can be represented as

$$T_k = (\Delta d_1^k, \Delta d_2^k, \dots, \Delta d_L^k), \quad (2)$$

where Δd_t^k is the displacement between P_t and P_{t+1} . The resulting vector is normalized by the sum of the magnitudes of the displacement vectors.

The improved version of dense trajectories [2] also takes the camera motion into account. It first gets the correspondence between two consecutive frames by SURF feature matching [29] and optical flow based matching. Then, the RANSAC [30] algorithm is used to estimate the homography matrix. Based on the homography, it rectifies the frame image to remove the camera motion and re-calculates the optical flow. In [1] and [2], HOG, HOF and MBH features are extracted along the dense trajectories, and different features are then encoded with Bag of Feature (BoF) or Fisher vector.

Unlike the original and improved versions of dense trajectories in [1] and [2], we only extract trajectories and represent them with their absolute coordinates. That is, given a video V , we obtain a set of trajectories

$$\mathbb{T}(V) = \{T_1, T_2, \dots, T_K\}, \quad (3)$$

where K is the number of trajectories, and T_k denotes the k^{th} trajectory

$$T_k = \{C_1^k, C_2^k, C_3^k, \dots, C_L^k\}, \quad (4)$$

$$C_l^k = (x_l^k, y_l^k, \Delta x_l^k, \Delta y_l^k), \quad (5)$$

where (x_l^k, y_l^k) is the spatial coordinate at l^{th} time step of the trajectory T_k , $(\Delta x_l^k, \Delta y_l^k)$ is the displacement between P_l and P_{l+1} along x and y axes. These trajectories will be used to construct sequential Trajectory Texture images and finally generate the descriptor with deep neural network, as described in the next section.

B. The Sequential Trajectory Texture Image

In most of existing action recognition approaches, the motion feature (e.g., HOF, MBH, temporal ConvNet feature) is vital for accurate recognition. However, extracting motion features for the actions which have long-term dependence will lead to very high computational overhead due to the processing of a large volume of video data. To address this problem, we propose a novel way to convert the motion information into two-dimensional space so that it can be efficiently processed.

Given a video V , we want to convert the motion in V to a set of images $\mathbb{I}(V)$. Towards this end, we first extract trajectories $\mathbb{T}(V)$ from this video, which are supposed to represent all movements. For trajectory T_k in $\mathbb{T}(V)$ and I_j in $\mathbb{I}(V)$, we convert T_k onto I_j as follows:

$$I_j(x, y) = \begin{cases} \sqrt{(\Delta x_l^k)^2 + (\Delta y_l^k)^2}, & \text{if } x_l^k = x \text{ and } y_l^k = y; \\ 0, & \text{otherwise.} \end{cases} \quad (6)$$

With Eq. (6), we are able to convert trajectories extracted from a segment of video into an image. We call it as Trajectory Texture image. However, because dense trajectories often overlap very much, there exist too many overwrites when generating the Trajectory Texture images, consequently leading to loss of recognition accuracy. To reduce the so-called overwriting problem, we further extend this equation to take the overwriting ratio into account. For image I_j , we define S_n^j and O_n^j as follows:

$$S_n^j(x, y) = 1, \text{ if } I_j(x, y) \neq 0, \quad (7)$$

$$O_n^j = O_{n-1}^j + \sum_{k=1}^K \sum_{l=1}^L S_n^j(x_l^k, y_l^k), \quad (8)$$

where $S_n^j(x, y)$ denotes whether it is set to a non-zero value in Trajectory Texture image I_j at position (x, y) after converting all trajectories starting from the n^{th} frame, and O_n^j is the number of pixels which are overwritten after the n^{th} frame.

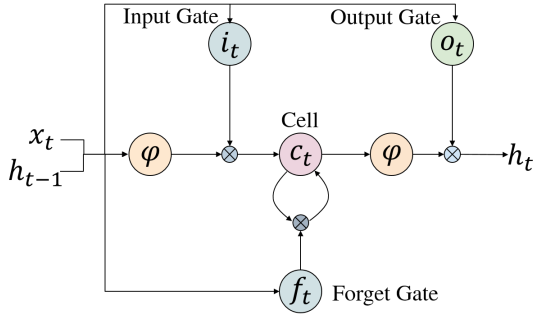


Fig. 3. Illustrating the LSTM unit used in this paper.

When O_n^j is larger than a threshold P , we start with a new Texture image and reset all variables.

Generally speaking, the performance of deep learning is highly related to the size of the training dataset. Labelling a large action recognition dataset and training a deep neural network from scratch is luxurious. Thus in recent years, a popular practice to train deep networks is to utilize the pre-trained models over the ImageNet dataset [3], [13], [15], [23]. In order to make Eq. (6) compatible with the existing ImageNet models, we re-formulate I_j to a three-channel image:

$$I_j(c, x_l^k, y_l^k) = \begin{cases} \Delta x_l^k, & c = 1; \\ \Delta y_l^k, & c = 2; \\ \sqrt{(\Delta x_l^k)^2 + (\Delta y_l^k)^2}, & c = 3. \end{cases} \quad (9)$$

where $I_j(c, x, y)$ is the pixel of I_j in the c^{th} channel at (x, y) , and (x_l^k, y_l^k) denotes all pixels in trajectory T_k . With this three-channel Trajectory Texture image, we are able to train our CNN model from the existing ImageNet model.

C. The Sequential Deep Convolutional Trajectory Descriptor

In this subsection, we will describe how to learn the sequential Deep Trajectory Descriptor (sDTD) from a set of Trajectory Texture images using deep neural network. In principle, any kind of CNNs can be adopted. In our implementation, we tested VGG-2048 [31] and GoogLeNet [16], and found that GoogLeNet was better than VGG-2048 in most cases.

Typically, a CNN is composed of multiple convolution layers, pooling layers and normalization layers, sometimes also includes some kinds of regularization (e.g., Dropout [32]). In the framework of action recognition, a CNN is usually used to learn spatial features. To learn spatial-temporal features, we instead use a CNN-RNN architecture [4]. As a special kind of RNNs, LSTMs are widely used to model temporal dependency and have been successfully applied to natural language processing, speech recognition, image and video description. In our network, we will use a simplified LSTM model [33], [34], which is illustrated in Figure 3.

Formally, given a sequence input as x_t (where $t \in T$, T is the range of time steps), an LSTM unit computes the output h_t by the following equations recursively:

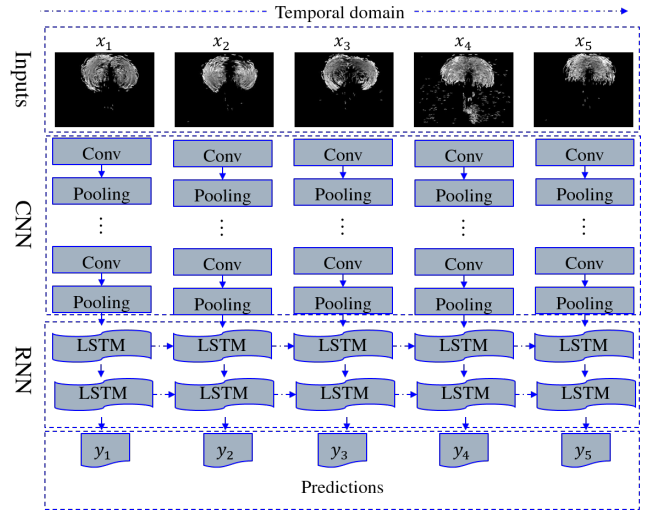


Fig. 4. The outputs of CNN are fed into LSTMs and the joint model is trained jointly. We will get a prediction for each frame and obtain the final prediction by fusing the predictions.

$$\begin{cases} i_t = \sigma(W_{xi}x_t + W_{hi}h_{t-1} + b_i), \\ f_t = \sigma(W_{xf}x_t + W_{hf}h_{t-1} + b_f), \\ c_t = f_t \odot c_{t-1} + i_t \odot \phi(W_{xc}x_t + W_{hc}h_{t-1} + b_c), \\ o_t = \sigma(W_{xo}x_t + W_{ho}h_{t-1} + b_o), \\ h_t = o_t \odot \phi(c_t), \end{cases} \quad (10)$$

where x_t and h_t are the input and hidden states for this LSTM unit at the t^{th} time step, i_t, f_t, c_t , and o_t are respectively the states of the input gate, forget gate, memory cell and output gate, W_{ab} is the weight matrix between gate a and gate b , b_a is the bias term of gate a , σ is the sigmoid nonlinearity, defined as $\sigma(x) = (1 + e^{-x})^{-1}$, which squashes real-valued inputs to a $(0, 1)$ range, and ϕ is the hyperbolic tangent nonlinearity, defined as $\phi(x) = \frac{e^x - e^{-x}}{e^x + e^{-x}} = 2\sigma(2x) - 1$.

To model temporal dependency, we feed the outputs of CNN into LSTMs. The joint model is shown in Figure 4. The whole network is composed of 4 parts: inputs, CNNs, RNNs and predictions. The CNN part contains convolutional layers, pooling layers, and fully-connected layers. The RNN part is a multi-layer RNN network which consists of multiple LSTM layers. With this CNN-RNN architecture, we are able to fuse spatial and temporal features, and get a prediction for each frame based on its previous frames. The implementation and training details will be described in Section IV.

III. ACTION RECOGNITION WITH SDTD

Basically, a good action recognition system should contain both spatial and temporal subsystems. In our model, we further consider the temporal subsystem as two modules: short-term temporal subsystem and long-term temporal subsystem. As a result, our three-stream framework includes spatial stream, temporal stream and sDTD stream.

The spatial stream is designed to capture static appearance features, by training on single frame images ($224 \times 224 \times 3$).

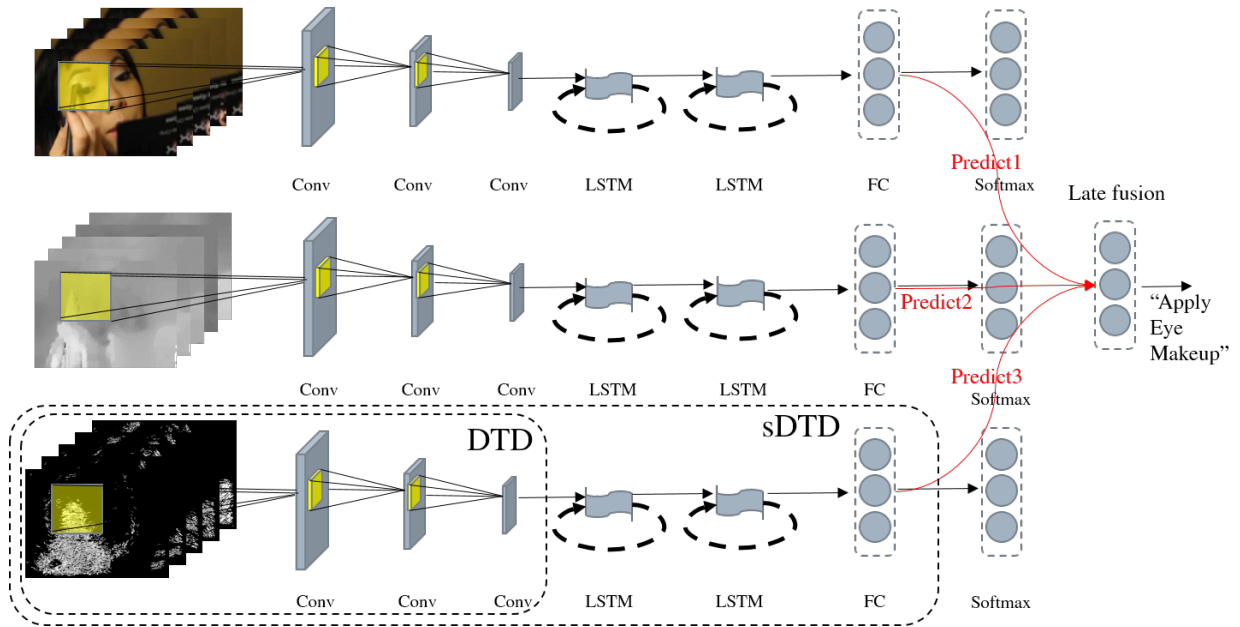


Fig. 5. Our three-stream framework for action recognition. This framework contains three streams: (i) the spatial stream for spatial feature, (ii) the temporal stream for short-term motion, (iii) the sDTD stream for long-term motion. All of the three streams have the same network architecture, which is composed of inputs, CNNs, RNNs and predictions. We do late fusion to get the final prediction for each video.

The temporal stream takes dense optical flow fields as inputs and aims to describe the short-term motion. Unlike the two-stream ConvNets in [3], whose temporal stream input is volumes of stacking optical flow fields ($224 \times 224 \times 2F$, where F is the number of stacking flows and is set to 10), our temporal stream input is single optical flow. An optical flow field is computed from two consecutive frames and composed of vertical and horizontal flows. To make use of the optical-flow-like images, we generate the pixel at (x, y) in the c^{th} channel of the t^{th} temporal inputs M_t , denoted as $M_t(c, x, y)$, as follows

$$M_t(c, x, y) = \begin{cases} u_t(x, y), & c = 1 \\ v_t(x, y), & c = 2 \\ \sqrt{u_t(x, y)^2 + v_t(x, y)^2}, & c = 3 \end{cases} \quad (11)$$

where u_t and v_t respectively are vertical and horizontal optical flows.

As mentioned in the previous subsection, the sDTD stream mainly focuses on modelling the long-term motion. Although both sDTD and the temporal stream utilize the optical flow fields which record the instantaneous motion state of the spatial space, they represent motion information in different manners. CNN in the temporal stream can learn the representation for short-term motion from several frames. On the contrary, sDTD samples the motion state sparsely (compared with the dense optical flow) for a video segment, and the temporal changes of spatial states result in the Trajectory Texture image, which is fed into the CNN so as to learn the representation of long-term motion. In short, the temporal stream can characterize short-term actions, while sDTD can describe long-term actions.

Finally, to get the final prediction, we apply late fusion to the three streams. Since there are three branches in GoogLeNet,

thus we will obtain three predictions for each stream. In order to take full advantage of GoogLeNet, we fuse nine predictions from three streams to get the final result.

IV. EXPERIMENTS

This section will first introduce the detail of datasets and their corresponding evaluation schemes. Then, we describe the implementation details of our method. Finally, we report the experimental results and compare sDTD with the state-of-the-art methods.

A. Datasets

To verify the effectiveness of sDTD, we conducted experiments on three public datasets, including KTH [35], HMDB51 [36] and UCF101 [37].

The KTH dataset contains 2,391 sequences that belong to six types of human actions by 25 subjects. These sequences are captured in four different scenarios with a homogeneous background. Following the original experimental setup, we divide the samples into the test set (9 subjects: 2, 3, 5, 6, 7, 8, 9, 10 and 22) and the training set (the remaining 16 subjects). Then we train the models on the training set and report the recognition accuracy on the test set over all classes.

The HMDB51 dataset is a large collection of realistic videos from various sources, including movies and web videos. It is composed of 6,766 video clips from 51 action categories, with each category containing at least 100 clips. Our experiments follow the original evaluation scheme, but only adopt the first training/testing split. In this split, each action class has 70 clips for training and 30 clips for testing.

The UCF101 dataset contains 13,320 video clips from 101 action classes and there are at least 100 video clips for each

class. We tested our model on the first training/testing split in the experiments.

Compared with the very large dataset used for image classification, the dataset for action recognition is relatively smaller. Therefore, we pre-trained our model on the ImageNet dataset [38]. As UCF101 is the largest one among the three datasets, we also used it to train our three-stream model initially, and then transferred the learnt model to KTH and HMDB51.

B. Implementation details

We used the Caffe toolbox [39] and the LSTM code in [4] to implement our model. As mentioned before, we tested our method with VGG-2048 [31] and GoogLeNet [16].

After initializing with the pre-trained ImageNet model for spatial and temporal streams, we trained our CNN-RNN network jointly. Because that sDTD will reduce the sample number for each video, it may fall in over-fitting if we train the CNN-RNN jointly in the sDTD stream. So in our implementation, we first trained a CNN model for sDTD and then added the RNN part. For KTH and HMDB51 datasets, we used the CNN-RNN model trained on the UCF101 split1 dataset and did not train the CNN separately.

The network weights were learnt using the mini-batch stochastic gradient descent with momentum (set to 0.9). The batch size for training the CNN model in the sDTD stream is 64. When training or testing a CNN-RNN model, we read 16 frames/flows/sDTDs from each video as one sample for the LSTM. For spatial and temporal streams, we read frames/flows with a stride of 5. Under this setting, we trained the CNN-RNN with a batch size of 16, which included 256 (16×16) frames/flows/sDTDs. We resized all input images to 340×256 , and then used the fixed-crop strategy [23] to crop a 224×224 region from images or their horizontal flips. Because the 16 consecutive samples were needed in the RNN, we also forced images from the same video to crop the same region. In the test phase, we sampled 4 corners and the center from each image and its horizontal flip, and 25 samples were extracted from each video.

For spatial stream, the learning rate started from 10^{-3} and was divided by 10 at iteration 30K and 50K, and training was stopped at 60K iterations. For temporal stream, we chose the TVL1 optical flow algorithm [40] and used the OpenCV GPU implementation. We discretized the optical flow fields into interval of $[0, 255]$ by a linear transformation and saved them as images. The learning rate was initially set as 10^{-3} and divided by 10 at iteration 80K and 100K. The training was stopped at 120K iteration. For sDTD stream, the learning rate for training CNN started from 10^{-3} and decreased to 10^{-4} after 30K iterations. It was then reduced to 10^{-5} after 50K iterations and training was stopped at 60K iteration. When training the CNN-RNN model, the learning rate started from 10^{-3} and was divided by 10 every 10K iterations, and training was stopped at 30K iteration.

C. Exploration experiments

Benefits from LSTMs. To evaluate the contribution of LSTMs, we firstly compared the performance of CNN and

TABLE I

Exploration of different network structures in sDTD on the UCF101 dataset. The subscripts V and G represent the VGG-2048 and GoogLeNet network structure. Here ConvNet denotes a pure CNN without LSTM layers. ST-ConvNet_G is the fusion model of spatial ConvNet_G and temporal ConvNet_G. Spatial and temporal streams are the first two streams in our three-stream framework, both of which have LSTM layers. DTD can be viewed as the sDTD without LSTM layers. ST-stream_G is the fusion model of spatial stream_G and temporal stream_G. LSTMs improve performance markedly in the three-stream framework, and GoogLeNet achieves better performance than VGG-2048.

model	Accuracy
Spatial ConvNet _G	79.0%
Temporal ConvNet _G	65.2%
Spatial stream _G	82.9%
Temporal stream _G	75.3%
DTD _V	70.7%
sDTD _V	70.9%
sDTD _G	71.7%
ST-ConvNet _G	85.5%
ST-stream _G	90.0%
ST-stream _G +DTD _V	90.9%
ST-stream _G +sDTD _V	91.8%
ST-stream _G +sDTD _G	92.1%

CNN-RNN on the UCF101 dataset. In this experiment, we trained the CNN with Trajectory Texture images and the resulting model was named as DTD. Then we trained the CNN-RNN based on DTD. We denote the two-stream model as ST-ConvNet_G, and ST-stream_G as the two-stream model with LSTM layers. The temporal ConvNet_G operates on 20 stacked optical flow images from 11 consecutive frames. In order to show their performance in the three-stream structure, we also fused them with the spatial stream and temporal stream. The results are shown in Table I. We can see that the temporal ConvNet_G gets the worst performance because no pre-trained model is available.

We can also find that the spatial and temporal streams outperform spatial and temporal ConvNets by 3.9% and 10.1% respectively, while the ST-stream_G is 4.5% better than ST-ConvNet_G. The remarkable improvements indicate that CNN-RNN is a better structure than the pure CNN. The DTD_V and sDTD_V get 70.7% and 70.9% respectively. It seems that LSTMs do not bring significant improvement for sDTD. However, when considering their performance in the three-stream structure, ST-stream_G+sDTD_V boost from ST-stream_G+DTD_V by about 1%. The reason may be that, LSTMs take more information into account so that sDTD can effectively encode long-term motion in the descriptor, which may be insufficient to recognize actions solely but is very informative to derive a correct prediction when fusing spatial and temporal streams. Thus, we use a CNN-RNN structure for the sDTD stream in the remainder of this section.

Network structure. Another important issue is the choice of network structure. We conducted an experiment on two networks: VGG-2048 and GoogLeNet and evaluated their three-stream performance on the UCF101 dataset. The results are shown in the Table I. We see that sDTD_G is about one percentage better than sDTD_V. The advantage of GoogLeNet decreases to 0.3 in the three-stream framework. However, this still proves the effectiveness of GoogLeNet. Therefore, in the

TABLE II

Exploration of the performance of different models on the UCF101 dataset. Our three streams are based on GoogLeNet. We compare our sDTD with iDT features [2] and two-stream ConvNets [3]. We also demonstrate the complementary properties of the three streams in the table.

Model	Accuracy
HOG [2], [41]	72.4%
HOF [2], [41]	76.0%
MBH [2], [41]	80.8%
HOF+MBH [2], [41]	82.2%
iDT [2], [41]	84.7%
Spatial stream ConvNet [3]	73.0%
Temporal stream ConvNet [3]	83.7%
Two-stream model (fusing by SVM) [3]	88.0%
Spatial stream	82.9%
Temporal stream	75.3%
sDTD	71.7%
ST-stream	90.0%
Spatial stream+sDTD	89.7%
Temporal stream+sDTD	82.5%
ST-stream+sDTD	92.1%

TABLE III

The performance of sDTD on the KTH, HMDB51 and UCF101 datasets. Our three-stream sDTD results are obtained by fusing all branches of GoogLeNet (note that GoogLeNet has three branches) in the three streams.

model	KTH	HMDB51	UCF101
sDTD	94.8%	41.1%	71.7%
ST-stream	93.7%	58.4%	90.0%
ST-stream+sDTD	96.8%	63.7%	92.1%
Final three-stream sDTD	96.8%	65.2%	92.2%

remainder of this section, we will use GoogLeNet to train our sDTD model and omit their subscripts.

Complementary properties of three streams. Finally, in order to get a good performance on action recognition, we investigated the complementary properties of the three streams on the UCF101 dataset. The results are summarized in Table II. We first fused the spatial stream and the temporal stream so as to obtain the ST-stream model. The ST-stream gets an accuracy of 90.0%, which is better than the two-stream model in [3]. This improvement comes from the use of GoogLeNet and LSTMs. The GoogLeNet learns better spatial features than the shallower network in [3], and LSTMs perform prediction based on the previous frames. The good performance of ST-stream means that the spatial stream and the temporal stream both benefit from each other. The accuracy achieves 89.7% when fusing the spatial stream with the sDTD stream, while gets 82.5% when fusing the temporal stream with the sDTD stream. We can thus conclude that the spatial, temporal and sDTD streams are complementary to each other. Finally, the accuracy of 92.2% for the three-stream model proves that their complementary properties can be utilized to improve the overall recognition performance.

D. Evaluation of sDTD

In this subsection, we aim to evaluate the performance of our sDTD on the KTH, HMDB51 and UCF101 datasets. The experimental results are summarized in Table III. We can see that, sDTD improves the ST-stream by 3.1% on KTH, 5.3% on HMDB51 and 2.1% on UCF101.

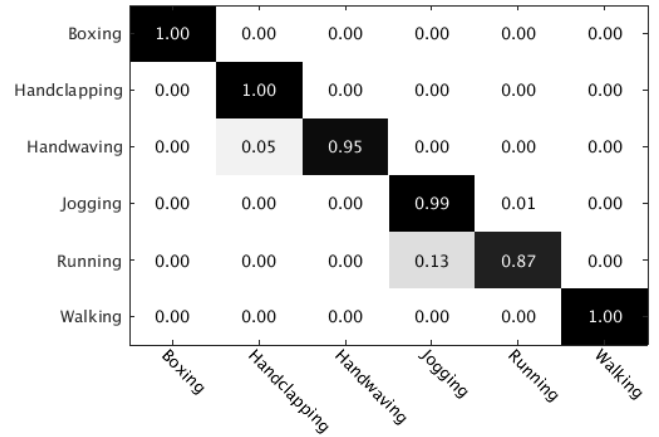


Fig. 8. Performance confusion matrix for our sDTD on the KTH dataset.

Figure 6 visualizes some examples of Trajectory Texture images. We can see that most background has been removed and the target object is successfully kept. And it is obvious that RGB images, optical flow fields and Trajectory Texture images can capture the visual information from different aspects, making the three streams complementary to each other.

In our method, each segment of a video can be converted into a few trajectory texture images (averagely 9 images in the UCF101 dataset). This can effectively reduce the number of images to be processed, consequently decreasing the computational efforts. In this way, our sDTD stream achieves a speed of 3.24 videos per second on the UCF101 dataset, which is fast enough for the real-time application.

As shown in Figure 7, we count the changes after fusing the sDTD stream into the ST-stream, and sDTD brings more changes to “Correct” than “Error”. A big value of “Correct”/“Error” means sDTD brings positive/negative effect on the ST-stream model, and zero means sDTD has no effect on the final prediction of that category. The circled parts are categories which sDTD has big effects on. As we can see, sDTD works well on *Running*, *Throwing* and *JumpRope* classes. Specifically, before fusing sDTD, all affected *Running* videos are mis-predicted as *Jogging*, most affected *Throwing* videos are mis-predicted as *Drawing*, while most affected *JumpRope* videos are mis-predicted as *Basketball*, *BodyWeightSquats* or *SoccerJuggling*. These actions are quite similar in frames or optical flow fields when no extra objects appearing, for example, basketball. However, their long-term motion has a lot difference so sDTD is able to classify them easily.

The confusion matrixes for sDTD on KTH, HMDB51 and UCF101 datasets are shown in Figure 8, 9 and 10. On the KTH dataset, our method performs perfectly on *Boxing*, *HandClapping* and *Walking* categories. The confusion matrix on the UCF101 dataset is also well diagonalized. However, the confusion matrix on the HMDB51 dataset shows that some categories are easily mis-classified, despite sDTD still performs well on most categories.

We then compare the performance of sDTD with iDT on the UCF101 dataset. They both make use of dense trajectories, but our sDTD outperforms iDT around 7.4%. We believe this

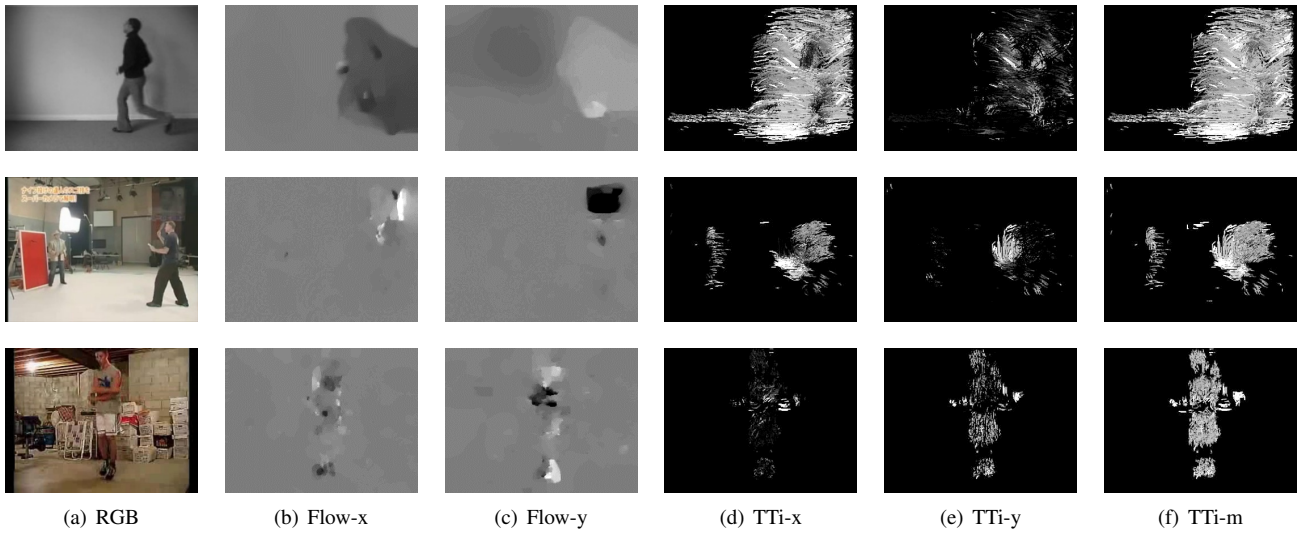


Fig. 6. Examples of video frames, optical flow fields, and three channels of Trajectory Texture images. Here TTI is the abbreviation of Trajectory Texture image. All images are modified to make them more visible.

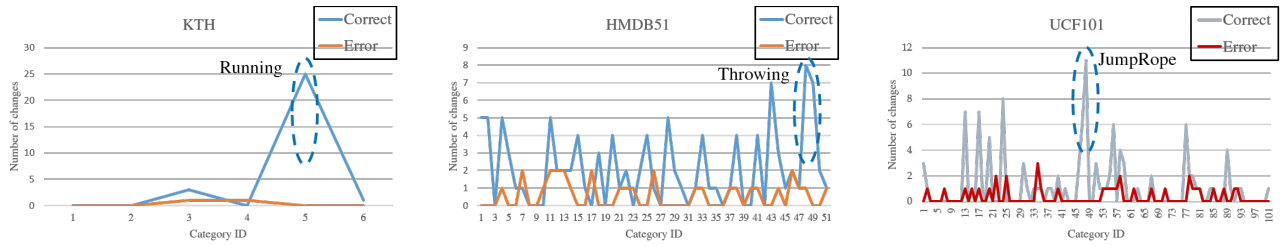


Fig. 7. Changes after fusing the sDTD stream into the ST-stream on the KTH, HMDB51 and UCF101 datasets. The x-axis and y-axis are category ID and the number of changed samples respectively. To get the changed samples, we simply compare the prediction results between the ST-stream and the three-streams. “Correct” (“Error”) means the number of videos that are predicted wrongly (correctly) before fusing the ST-stream, but correctly (wrongly) predicted with the ST-stream.

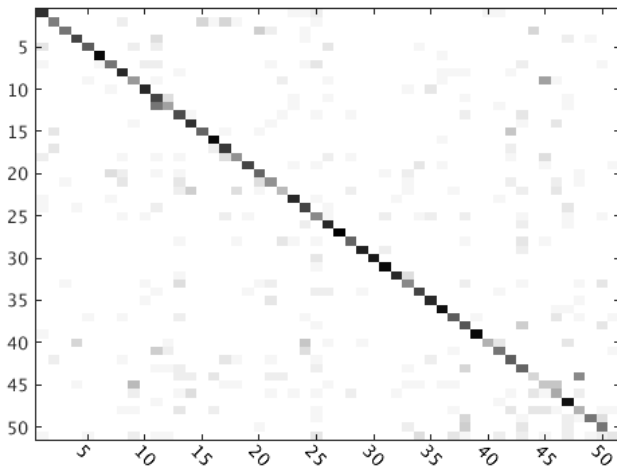


Fig. 9. Performance confusion matrix for our sDTD on the HMDB51 dataset.

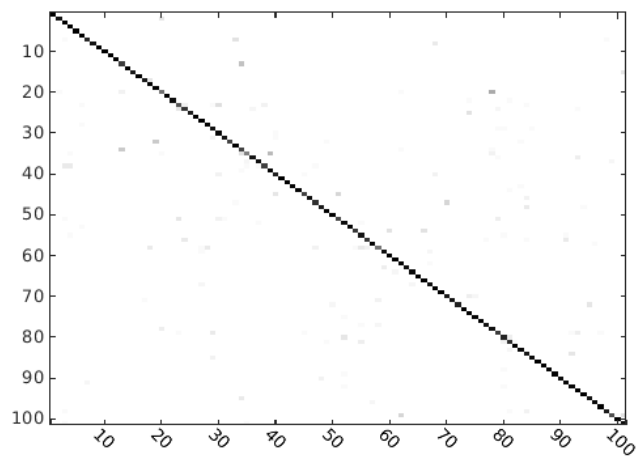


Fig. 10. Performance confusion matrix for our sDTD on the UCF101 dataset.

mostly attributes to the power of deep neural network and our three-stream framework.

Finally, we compare our sDTD with DTD in [19]. The single sDTD stream achieves comparable performance with DTD+iDT on the KTH dataset, and surpasses it after fusing

the spatial and temporal streams.

E. Comparison to the state of the art

Table IV compares our recognition results with several state-of-the-art methods on the KTH, HMDB51 and UCF101

TABLE IV
Comparison of sDTD to the state-of-the-art methods.

KTH		HMDB51		UCF101	
HOG+HoF+BoF [42]	91.8%	STIP+BoF [36]	23.0%	STIP+BoF [36]	43.9%
Class-specific vocabularies [43]	94.5%	Motionlets [44]	42.1%	Deep Net [45]	63.3%
Hierarchical Mined [46]	95.7%	DT+BoF [47]	46.6%	DT+VLAD [48]	79.9%
ISA network [49]	93.9%	DT+MVSV [48]	55.9%	DT+MVSV [48]	83.5%
DT+BoF [1]	94.2%	iDT+FV [2]	57.2%	iDT+FV [41]	85.9%
Dynamic coordinate system [50]	94.9%	iDT+HSV [51]	61.1%	iDT+HSV [51]	88.0%
PMF+AdaBoost+Correlogram+SVM [52]	95.5%	PMF+AdaBoost+Correlogram+SVM [52]	36.5%	Hybrid deep framework [13]	91.3%
Scene Context descriptor [53]	89.8%	Two-stream model [23]	59.4%	Two-stream model [23]	88.0%
3D \mathcal{R} Transform [54]	95.5%	$F_{ST}CN$ [55]	59.1%	$F_{ST}CN$ [55]	88.1%
DTD+iDT [19]	95.6%	TDD+FV [15]	63.2%	TDD+FV [15]	90.3%
-	-	TDD+iDT+FV [15]	65.9%	TDD+iDT+FV [15]	91.5%
-	-	Visual Attention [27]	41.3%	Very deep two-stream [23]	91.4%
-	-	-	-	LSTM with 30 Frame Unroll [26]	88.6%
Three-stream sDTD	96.8%	Three-stream sDTD	65.2%	Three-stream sDTD	92.2%

datasets. The performance of sDTD outperforms these methods on the KTH and UCF101 datasets, and outperforms most methods on the HMDB51 dataset. Unlike most of purely hand-crafted features or deep models, the work [15] uses a TDD+iDT+FV framework, which takes deep feature and hand-crafted feature into one model. Our model still outperforms [15] by 0.7% on the UCF101 dataset. This validates the effectiveness of our sDTD.

V. CONCLUSIONS

This paper has proposed an effective descriptor for long-term actions, sDTD. A three-stream framework is then employed to identify actions from a video sequence. Our method achieve state-of-the-art performance on the KTH and UCF101 datasets, and outperforms most of existing methods on the HMDB51 dataset. In addition, the performance should be further improved by fusing the hand-crafted features like iDT.

ACKNOWLEDGMENT

This work is partially supported by grants from the National Basic Research Program of China under grant 2015CB351806, the National Natural Science Foundation of China under contract No. 61390515, No. 61425025 and No. 61471042, the National Key Technology Research and Development Program under contract No. 2014BAK10B02 and Beijing Municipal Commission of Science and Technology under contract No. Z151100000915070, and Shenzhen Peacock Plan.

REFERENCES

- [1] H. Wang, A. Kläser, C. Schmid, and C.-L. Liu, "Action recognition by dense trajectories," in *Proceedings of IEEE Conference on Computer Vision and Pattern Recognition*, 2011, pp. 3169–3176.
- [2] H. Wang and C. Schmid, "Action recognition with improved trajectories," in *Proceedings of IEEE International Conference on Computer Vision*, 2013, pp. 3551–3558.
- [3] K. Simonyan and A. Zisserman, "Two-stream convolutional networks for action recognition in videos," in *Advances in Neural Information Processing Systems*, 2014, pp. 568–576.
- [4] J. Donahue, L. Anne Hendricks, S. Guadarrama, M. Rohrbach, S. Venugopalan, K. Saenko, and T. Darrell, "Long-term recurrent convolutional networks for visual recognition and description," in *Proceedings of IEEE Conference on Computer Vision and Pattern Recognition*, 2015, pp. 2625–2634.
- [5] D. G. Lowe, "Distinctive image features from scale-invariant keypoints," *International Journal of Computer Vision*, vol. 60, no. 2, pp. 91–110, 2004.
- [6] P. Scovanner, S. Ali, and M. Shah, "A 3-dimensional sift descriptor and its application to action recognition," in *Proceedings of the 15th ACM International Conference on Multimedia*, 2007, pp. 357–360.
- [7] R. Poppe, "A survey on vision-based human action recognition," *Image and Vision Computing*, vol. 28, no. 6, pp. 976–990, 2010.
- [8] N. Dalal and B. Triggs, "Histograms of oriented gradients for human detection," in *Proceedings of IEEE Conference on Computer Vision and Pattern Recognition*, vol. 1, 2005, pp. 886–893.
- [9] N. Dalal, B. Triggs, and C. Schmid, "Human detection using oriented histograms of flow and appearance," in *Proceedings of European Conference on Computer Vision*. Springer, 2006, pp. 428–441.
- [10] F. Perronnin, J. Sánchez, and T. Mensink, "Improving the fisher kernel for large-scale image classification," in *Proceedings of European Conference on Computer Vision*. Springer, 2010, pp. 143–156.
- [11] Z. Zhou, F. Shi, and W. Wu, "Learning spatial and temporal extents of human actions for action detection," *IEEE Transactions on Multimedia*, vol. 17, no. 4, pp. 512–525, 2015.
- [12] K. He, X. Zhang, S. Ren, and J. Sun, "Deep residual learning for image recognition," *arXiv preprint arXiv:1512.03385*, 2015.
- [13] Z. Wu, X. Wang, Y.-G. Jiang, H. Ye, and X. Xue, "Modeling spatial-temporal clues in a hybrid deep learning framework for video classification," in *Proceedings of the 23rd ACM international conference on Multimedia*, 2015, pp. 461–470.
- [14] I. Sutskever, O. Vinyals, and Q. V. Le, "Sequence to sequence learning with neural networks," in *Advances in neural information processing systems*, 2014, pp. 3104–3112.
- [15] L. Wang, Y. Qiao, and X. Tang, "Action recognition with trajectory-pooled deep-convolutional descriptors," in *Proceedings of IEEE Conference on Computer Vision and Pattern Recognition*, 2015, pp. 4305–4314.
- [16] C. Szegedy, W. Liu, Y. Jia, P. Sermanet, S. Reed, D. Anguelov, D. Erhan, V. Vanhoucke, and A. Rabinovich, "Going deeper with convolutions," in *Proceedings of IEEE Conference on Computer Vision and Pattern Recognition*, 2015, pp. 1–9.
- [17] K. He, X. Zhang, S. Ren, and J. Sun, "Delving deep into rectifiers: Surpassing human-level performance on imagenet classification," in *Proceedings of the IEEE International Conference on Computer Vision*, 2015, pp. 1026–1034.
- [18] G. E. Dahl, D. Yu, L. Deng, and A. Acero, "Context-dependent pre-trained deep neural networks for large-vocabulary speech recognition," *IEEE Transactions on Audio, Speech, and Language Processing*, vol. 20, no. 1, pp. 30–42, 2012.
- [19] Y. Shi, W. Zeng, T. Huang, and Y. Wang, "Learning deep trajectory descriptor for action recognition in videos using deep neural networks," in *Proceedings of IEEE International Conference on Multimedia and Expo*, 2015, pp. 1–6.
- [20] Z. Wu, Y.-G. Jiang, J. Wang, J. Pu, and X. Xue, "Exploring inter-feature and inter-class relationships with deep neural networks for video classification," in *Proceedings of the 22nd ACM International Conference on Multimedia*, 2014, pp. 167–176.
- [21] S. Zha, F. Luisier, W. Andrews, N. Srivastava, and R. Salakhutdinov, "Exploiting image-trained cnn architectures for unconstrained video classification," *arXiv preprint arXiv:1503.04144*, 2015.

- [22] S. Ji, W. Xu, M. Yang, and K. Yu, "3d convolutional neural networks for human action recognition," *IEEE Transactions on Pattern Analysis and Machine Intelligence*, vol. 35, no. 1, pp. 221–231, 2013.
- [23] L. Wang, Y. Xiong, Z. Wang, and Y. Qiao, "Towards good practices for very deep two-stream convnets," *arXiv preprint arXiv:1507.02159*, 2015.
- [24] M. Hasan and A. K. Roy-Chowdhury, "A continuous learning framework for activity recognition using deep hybrid feature models," *IEEE Transactions on Multimedia*, vol. 17, no. 11, pp. 1909–1922, 2015.
- [25] L. Pang, S. Zhu, and C.-W. Ngo, "Deep multimodal learning for affective analysis and retrieval," *IEEE Transactions on Multimedia*, vol. 17, no. 11, pp. 2008–2020, 2015.
- [26] J. Yue-Hei Ng, M. Hausknecht, S. Vijayanarasimhan, O. Vinyals, R. Monga, and G. Toderici, "Beyond short snippets: Deep networks for video classification," in *Proceedings of IEEE Conference on Computer Vision and Pattern Recognition*, 2015, pp. 4694–4702.
- [27] S. Sharma, R. Kiroso, and R. Salakhutdinov, "Action recognition using visual attention," *arXiv preprint arXiv:1511.04119*, 2015.
- [28] W. Zaremba and I. Sutskever, "Learning to execute," *arXiv preprint arXiv:1410.4615*, 2014.
- [29] H. Bay, T. Tuytelaars, and L. Van Gool, "Surf: Speeded up robust features," in *Proceedings of European Conference on Computer Vision*. Springer, 2006, pp. 404–417.
- [30] M. A. Fischler and R. C. Bolles, "Random sample consensus: a paradigm for model fitting with applications to image analysis and automated cartography," *Communications of the ACM*, vol. 24, no. 6, pp. 381–395, 1981.
- [31] K. Chatfield, K. Simonyan, A. Vedaldi, and A. Zisserman, "Return of the devil in the details: Delving deep into convolutional nets," *Proceedings of British Machine Vision Conference*, 2014.
- [32] G. E. Hinton, N. Srivastava, A. Krizhevsky, I. Sutskever, and R. R. Salakhutdinov, "Improving neural networks by preventing co-adaptation of feature detectors," *arXiv preprint arXiv:1207.0580*, 2012.
- [33] A. Graves, A.-r. Mohamed, and G. Hinton, "Speech recognition with deep recurrent neural networks," in *Proceedings of IEEE International Conference on Acoustics, Speech and Signal Processing*, 2013, pp. 6645–6649.
- [34] S. Hochreiter and J. Schmidhuber, "Long short-term memory," *Neural computation*, vol. 9, no. 8, pp. 1735–1780, 1997.
- [35] C. Schödl, I. Laptev, and B. Caputo, "Recognizing human actions: a local svm approach," in *Proceedings of the 17th International Conference on Pattern Recognition*, vol. 3, 2004, pp. 32–36.
- [36] H. Kuehne, H. Jhuang, E. Garrote, T. Poggio, and T. Serre, "Hmdb: a large video database for human motion recognition," in *Proceedings of IEEE International Conference on Computer Vision*, 2011, pp. 2556–2563.
- [37] K. Soomro, A. R. Zamir, and M. Shah, "Ucf101: A dataset of 101 human actions classes from videos in the wild," *arXiv preprint arXiv:1212.0402*, 2012.
- [38] J. Deng, W. Dong, R. Socher, L.-J. Li, K. Li, and L. Fei-Fei, "Imagenet: A large-scale hierarchical image database," in *Proceedings of IEEE Conference on Computer Vision and Pattern Recognition*, 2009, pp. 248–255.
- [39] Y. Jia, E. Shelhamer, J. Donahue, S. Karayev, J. Long, R. Girshick, S. Guadarrama, and T. Darrell, "Caffe: Convolutional architecture for fast feature embedding," in *Proceedings of the ACM International Conference on Multimedia*, 2014, pp. 675–678.
- [40] C. Zach, T. Pock, and H. Bischof, "A duality based approach for realtime tv-l1 optical flow," in *Pattern Recognition*. Springer, 2007, pp. 214–223.
- [41] H. Wang and C. Schmid, "Learn-inria submission for the thumos workshop," in *Proceedings of ICCV workshop on action recognition with a large number of classes*, vol. 2, no. 7, 2013, p. 8.
- [42] I. Laptev, M. Marszalek, C. Schmid, and B. Rozenfeld, "Learning realistic human actions from movies," in *Proceedings of IEEE Conference on Computer Vision and Pattern Recognition*, 2008, pp. 1–8.
- [43] A. Kovashka and K. Grauman, "Learning a hierarchy of discriminative space-time neighborhood features for human action recognition," in *Proceedings of IEEE Conference on Computer Vision and Pattern Recognition*, 2010, pp. 2046–2053.
- [44] L. Wang, Y. Qiao, and X. Tang, "Motionlets: Mid-level 3d parts for human motion recognition," in *Proceedings of IEEE Conference on Computer Vision and Pattern Recognition*, 2013, pp. 2674–2681.
- [45] A. Karpathy, G. Toderici, S. Shetty, T. Leung, R. Sukthankar, and L. Fei-Fei, "Large-scale video classification with convolutional neural networks," in *Proceedings of IEEE conference on Computer Vision and Pattern Recognition*, 2014, pp. 1725–1732.
- [46] A. Gilbert, J. Illingworth, and R. Bowden, "Action recognition using mined hierarchical compound features," *IEEE Transactions on Pattern Analysis and Machine Intelligence*, vol. 33, no. 5, pp. 883–897, 2011.
- [47] H. Wang, A. Kläser, C. Schmid, and C.-L. Liu, "Dense trajectories and motion boundary descriptors for action recognition," *International Journal of Computer Vision*, vol. 103, no. 1, pp. 60–79, 2013.
- [48] Z. Cai, L. Wang, X. Peng, and Y. Qiao, "Multi-view super vector for action recognition," in *Proceedings of IEEE conference on Computer Vision and Pattern Recognition*, 2014, pp. 596–603.
- [49] Q. V. Le, W. Y. Zou, S. Y. Yeung, and A. Y. Ng, "Learning hierarchical invariant spatio-temporal features for action recognition with independent subspace analysis," in *Proceedings of IEEE Conference on Computer Vision and Pattern Recognition*, 2011, pp. 3361–3368.
- [50] P. Bilinski, E. Corvee, S. Bak, and F. Bremond, "Relative dense tracklets for human action recognition," in *Proceedings of the 10th IEEE International Conference and Workshops on Automatic Face and Gesture Recognition*, 2013, pp. 1–7.
- [51] X. Peng, L. Wang, X. Wang, and Y. Qiao, "Bag of visual words and fusion methods for action recognition: Comprehensive study and good practice," *Computer Vision and Image Understanding*, 2016.
- [52] L. Liu, L. Shao, and P. Rockett, "Boosted key-frame selection and correlated pyramidal motion-feature representation for human action recognition," *Pattern recognition*, vol. 46, no. 7, pp. 1810–1818, 2013.
- [53] K. K. Reddy and M. Shah, "Recognizing 50 human action categories of web videos," *Machine Vision and Applications*, vol. 24, no. 5, pp. 971–981, 2013.
- [54] C. Yuan, X. Li, W. Hu, H. Ling, and S. Maybank, "3d r transform on spatio-temporal interest points for action recognition," in *Proceedings of IEEE Conference on Computer Vision and Pattern Recognition*, 2013, pp. 724–730.
- [55] L. Sun, K. Jia, D.-Y. Yeung, and B. E. Shi, "Human action recognition using factorized spatio-temporal convolutional networks," in *Proceedings of the IEEE International Conference on Computer Vision*, 2015, pp. 4597–4605.